PROCEEDINGS OF SCIENCE

# Photometry of blazars using the Las Cumbres Observatory robotic telescope network

**Hartmut Winkler,**[a,*] **Dylan Morgan**[b] **and Francois van Wyk**[a]

[a] *Department of Physics, University of Johannesburg, Kingsway, Auckland Park, Johannesburg, South Africa*

[b] *Department of Physics, University of Durham, South Road, Durham DH1 3LE, United Kingdom*

*E-mail:* hwinkler@uj.ac.za, dthembamorgan@gmail.com, fvw@saao.ac.za

We present an analysis of the photometry of nine of the brightest blazars using the 0.4m robotic telescopes of the Las Cumbres Observatory global network. Observations were carried out in four filters (B, V and Sloan g and r) with a typical cadence of 1 month over periods spanning 1-2 years. Almost all of the targets showed substantial variations over the period of investigation, in some cases by over a magnitude. In particular, the prototype BL Lac went through its most luminous recorded phase to date in late 2022, an event that was also monitored in high energy wave bands by other researchers. We determined the colour of the variable component using the flux variation gradient method, and hence establish the flux distribution of the variable source by isolating this component from the host galaxy background. We confirm that blazars occupy a characteristic zone in specific flux vs. flux diagrams. Finally, we examine optical spectra of some of our targets, some of which we obtained at SAAO. We explore the relationship between the optical spectral characteristics and the photometric behaviour.

*High Energy Astrophysics in Southern Africa 2023 (HEASA 2023)*
*September 5 - 9, 2023*
*Mtunzini, KwaZulu-Natal, South Africa*

*Speaker





PoS(HEASA2023)007

## 1. Introduction

The measurement and analysis of the spectral energy distribution provides a critical test of the presence and relative strength of the various components contributing to a blazar's total flux.

Throughout its x-ray and gamma ray regime, a blazar spectrum is dominated by a strong component usually ascribed to inverse Compton radiation [1]. At the opposite (low frequency) radio end, a blazar's flux distribution generally displays a synchrotron component that is, as with inverse Compton radiation, also usually associated with a jet. This component typically remains prominent through the infrared region and can often also clearly be detected in the optical.

The isolation of these components, which can overlap in the optical and adjacent wavebands, can however be complicated by the presence of other substantial components. These are (i) thermal emission from the accretion disk and other hot regions in the immediate surrounds of the black hole, (ii) thermal emission from warm dust and other gas clouds associated with the dust torus and narrow line regions, and (iii) emission lines and bands linked to atomic line transitions involving especially H I and Fe II (e.g. [2]). To complicate matters further, ultraviolet and optical photons from the AGN are particularly susceptible to attenuation due to interstellar gas and dust, both in the Milky Way and in the AGN host galaxy. Section 3 will describe how the analysis of photometric variations offers a means to isolate the synchrotron component from these other contributors.

Blazars also display a variety of optical spectra, some with featureless blue continua characteristic of the BL Lac objects, while others may include a host galaxy component and even emission lines (see, e.g. [3]). Previous investigations suggest a relationship between the blazar class and the shape and frequency range of the synchrotron spectrum [1].

## 2. Spectroscopy

The objects selected for this study include most of the brightest BL Lac objects in the sky, as well as two further radio-loud AGN (NGC 1275 and PKS 0521−365) that have historically displayed strong optical variability. The observed sample and known spectroscopic details thereof are listed in Table 1.

| Name | RA(2000) | Dec(2000) | $z$ | Roma BZCAT | Reference |
|---|---|---|---|---|---|
| NGC 1275 | 03 19 48.2 | +41 30 42 | 0.0176 | uncertain class | [4, 5] |
| PKS 0521−365 | 05 22 58.0 | −36 27 31 | 0.0554 | uncertain class | [6, 7] |
| Mkn 421 | 11 04 27.3 | +38 12 32 | 0.0300 | BL Lac | [3] |
| Mkn 180 | 11 36 26.4 | +70 09 27 | 0.0453 | BL Lac | [8] |
| AP Lib | 15 17 41.8 | −24 22 19 | 0.0491 | BL Lac | [6, 9] |
| Mkn 501 | 16 53 52.2 | +39 45 36 | 0.0337 | BL Lac | [3, 5] |
| PKS 2005−489 | 20 09 25.4 | −48 49 54 | 0.0710 | BL Lac | [6, 7] |
| PKS 2155−304 | 21 58 52.1 | −30 13 32 | 0.1167 | BL Lac | [6, 7] |
| BL Lac | 22 02 43.3 | +42 16 40 | 0.0686 | BL Lac | [5] |

**Table 1:** Coordinates, redshift, blazar class (according to the Roma BZCAT catalogue[10]) and references to studies where the optical spectra are displayed.

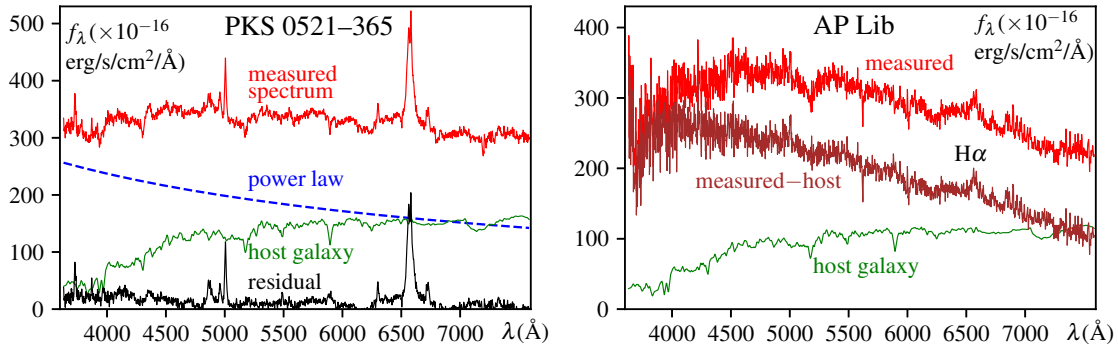


**Figure 1:** SAAO spectra of PKS 0521−365 and AP Lib. Also shown are the adopted host galaxy and power law components. The left plot also shows the residual emission line spectrum of PKS 0521−365 obtained after subtracting the power law and host galaxy contributions from the measured spectrum. No good single power law fit could be identified for AP Lib.

Further spectroscopic observations of PKS 0521−365 and AP Lib were carried out with the SpUpNIC spectrograph [11] on the 1.9 m telescope at the Sutherland station of the South African Astronomical Observatory on 22 Nov 2022 and 28 Aug 2023, respectively. Two integrations of 1200 s were collected per object, and the processing, wavelength and flux calibration, redshift determination and correction for extinction in our Galaxy of these spectra was carried out in an identical manner to spectra published previously by two of us (see [12] for exact details).

Even though the 2.7″ slit width used excludes much contaminating extra-nuclear starlight from the AGN host galaxy, a substantial fraction of the photons recorded in optical spectral observations are attributable to this component. Attempts were made to fit the measured spectral continuum as the combination of a host galaxy template and a single power law of the form

$$f_\nu \propto \nu^\alpha.$$

where $\nu$ is the frequency and $\alpha$ is the power law index. Such a power law is commonly used for modeling AGN spectral continua as this relationship mathematically approximates the low-frequency tail of a blackbody curve as well as a synchrotron spectrum.

## 3. Photometry

Photometric measurements in the Johnson B & V and Sloan g & r filters were performed using the 0.4 m telescope network of the Las Cumbres Observatory (LCO) [13] between Nov 2021 and Sep 2023, with additional points collected for some targets up to Jan 2024 in order to further reduce the uncertainty.

Images obtained by LCO are automatically processed through a photometry pipeline named BANZAI. Photometric measurements were carried out by projecting circular apertures with a radius of 3″ centered on each object identified by the source extractor used within BANZAI. The conversion to standard magnitudes was carried out with the aid of the APASS photometric database [14], where most stars down to roughly $V = 17$ in our frames have determined B, V, g and r filter magnitudes.

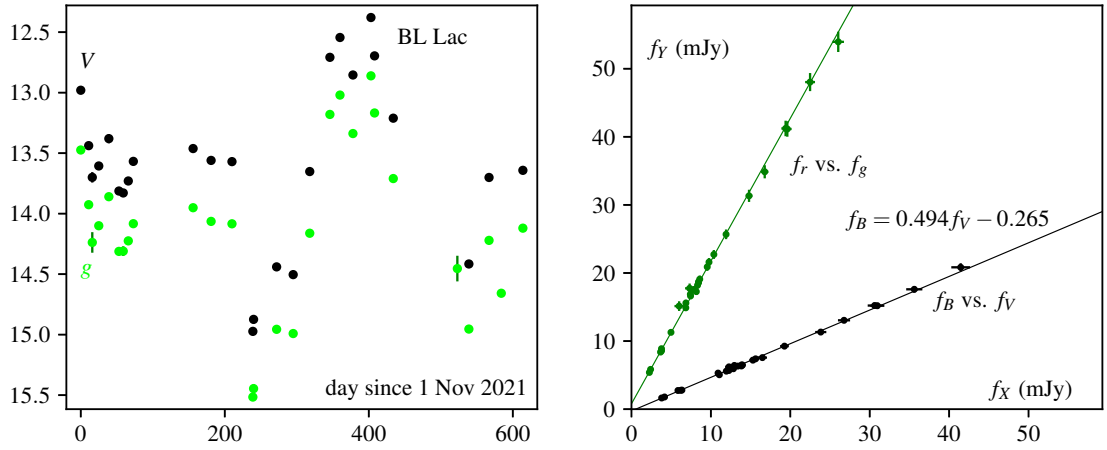


**Figure 2:** The left panel illustrates the dramatically varying V- and g'band light curves of BL Lac over the two-year period between November 2021 and September 2023. The right panel displays the flux variation gradient plots of LCO BVgr photometric measurements of BL Lac. The solid lines represent the best linear fits to the $f_B$ vs. $f_V$ and $f_r$ vs. $f_g$ plots.

Up to mid-2023 these telescopes were fitted with SBIG cameras. Images recorded with these detectors required a correction to mitigate against non-linear count rates reported by LCO. The procedure used to achieve this will be described more fully in a future publication.

The colours of the variable component were determined by means of the flux variation gradient (FVG) method [15]. This procedure utilises the fact that plots of the fluxes in one filter are related by a tight linear relationship to the fluxes in another filter. The slope of this line can be converted directly back to the nuclear colour. These, as well as the associated uncertainties and spectral indexes, are listed in Table 2, and the results are compared to Seyfert galaxies in Fig. 3. These variable component colours can also be employed as an indicator of reddening and extinction. Note that while in Fig. 2 the linear fits seem to skirt the origin, this will not be the case when the host galaxy colour differs considerably from the variable component colour; in that event this technique can be used to separate the host galaxy contribution from the variable nucleus (see [15] for a more comprehensive explanation).

## 4. Discussion

The AGN investigated here occupy a well-defined region on the $g-r$ vs. $B-V$ plots in Fig. 3. Their location in these diagram is distinct from where the concentration of Seyfert galaxies may be found near $B-V = 0.1$, $g-r = 0.0$, which likely corresponds to unobscured AGN with broad-line Seyfert spectra. The Seyferts further towards the top right corner of the plot are those with obscured nuclei. While the colours of the blazars are not very different to those of a Seyfert with a reddening of $E(B-V) \sim 0.5$, they appear slightly displaced from where one would find the Seyfert reddening vector. Colour differences between blazars are more likely a reflection of different synchrotron component shapes rather than reddening, as optical spectra of the blazars invariably show enhanced flux at the blue end of the optical spectrum, the region most prone to extinction losses.

| Name | No. Obs. | $B-V$ | $\sigma_{B-V}$ | $g-r$ | $\sigma_{g-r}$ | $\alpha$(B-V) | $\alpha$(g-r) |
|---|---|---|---|---|---|---|---|
| NGC 1275 | 26 | 0.47 | 0.03 | 0.32 | 0.04 | −1.5 | −1.1 |
| PKS 0521−365 | 11 | 0.52 | 0.08 | 0.47 | 0.08 | −1.7 | −1.6 |
| Mkn 421 | 20 | 0.25 | 0.03 | 0.09 | 0.03 | −0.6 | −0.3 |
| Mkn 180 | 21 | 0.44 | 0.06 | 0.17 | 0.06 | −1.3 | −0.6 |
| AP Lib | 25 | 0.48 | 0.02 | 0.39 | 0.02 | −1.5 | −1.3 |
| Mkn 501 | 20 | 0.27 | 0.16 | 0.29 | 0.15 | −0.6 | −1.0 |
| PKS 2005−489 | 22 | 0.29 | 0.03 | 0.20 | 0.03 | −0.7 | −0.7 |
| PKS 2155−304 | 22 | 0.41 | 0.02 | 0.30 | 0.02 | −1.2 | −1.0 |
| BL Lac | 28 | 0.58 | 0.01 | 0.52 | 0.01 | −1.9 | −1.7 |

**Table 2:** Optical nuclear colours and corresponding spectral power indexes.

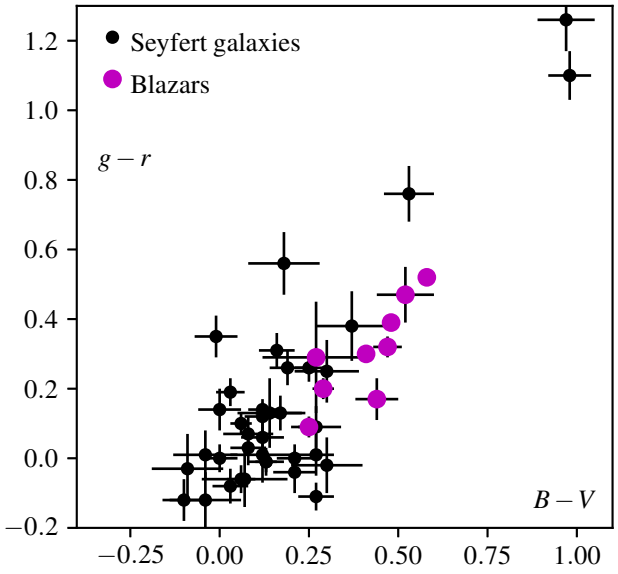


**Figure 3:** Plots of $g-r$ vs. $B-V$ for the variable component of the nine AGN investigated in this study. The positions of well-determined variable components of Seyfert galaxies determined in a related programme (Winkler, in preparation) are plotted for comparison.

We are unable to confirm a systematic difference between the nuclear colours of BL Lac objects and objects labeled as "uncertain class" in the Roma catalogue. We note that the two objects in question, NGC 1275 and PKS 0521−365, are strong radio emitters and have Seyfert-like emission lines, meaning that they may also be classified as radio-loud Seyfert. So their synchrotron peak is located at a similar frequency as for several archetypal BL Lac objects (including BL Lac itself).

The spectral indexes we derive are consistent with previous determinations. The comprehensive study of the spectral energy distribution of blazars by [1] identified synchrotron emission peak positions ranging all the way from the infrared to the ultraviolet. They found the synchrotron peak of Mkn 421 to be in the extreme ultraviolet, while the corresponding peaks of BL Lac, AP Lib and PKS 2155−304 were identified to be in the infrared. We confirm the same result from our much

more recent observations.

Finally, we draw attention to the dramatic brightening of BL Lac near the end of 2022. The photometric measurements recorded around that time correspond to the most luminous states witnessed to date [16].

## 5. Conclusion

The spectral index of the variable component at optical wavebands has been determined for nine bright blazars. For all objects observed, the variability largely stems from the synchrotron component, and our application of the flux variation gradient technique has allowed us to remove optical contamination due to the host galaxy. Even though there appears to be a bluer accretion disk component in some objects, any variation of this component has been minimal compared to the synchrotron part. In all objects the synchrotron component drops off with increasing frequency in the optical. The drop-off is steeper in some objects than others, which not only allows one to identify whether specific objects are low- or high-synchrotron peaked, but we also exactly quantify the spectral shape of the synchrotron component in the optical regime. If there are future deviations from the linear relationships we identified in the various flux-flux plots then that would signify a remarkable change in the synchrotron peak position.

## Acknowledgements

This paper uses observations made from the South African Astronomical Observatory (SAAO) and makes use of observations from the Las Cumbres Observatory global telescope network. This research has made use of the NASA/IPAC Extragalactic Database (NED), which is funded by the National Aeronautics and Space Administration and operated by the California Institute of Technology, as well as the AAVSO Photometric All-Sky Survey (APASS), funded by the Robert Martin Ayers Sciences Fund and NSF AST-1412587.

## References

[1] A. A. Abdo, M. Ackermann, I. Agudo, M. Ajello, H. D. Aller, M. F. Aller et al., *The Spectral Energy Distribution of Fermi Bright Blazars*, *Astrophys. J.* **716** (2010) 30.

[2] R. A. Edelson and M. A. Malkan, *Spectral Energy Distributions of Active Galactic Nuclei between 0.1 and 100 Microns*, *Astrophys. J.* **308** (1986) 59.

[3] M. J. M. Marcha, I. W. A. Browne, C. D. Impey and P. S. Smith, *Optical spectroscopy and polarization of a new sample of optically bright flat radio spectrum sources*, *Mon. Not. R. astr. Soc.* **281** (1996) 425.

[4] R. C. J. Kennicutt, *A Spectrophotometric Atlas of Galaxies*, *Astrophys. J. Suppl.* **79** (1992) 255.

[5] C. R. Lawrence, J. R. Zucker, A. C. S. Readhead, S. C. Unwin, T. J. Pearson and W. Xu, *Optical Spectra of a Complete Sample of Radio Sources. I. The Spectra*, *Astrophys. J. Suppl.* **107** (1996) 541.

[6] R. Falomo, R. Scarpa and M. Bersanelli, *Optical Spectrophotometry of Blazars*, *Astrophys. J. Suppl.* **93** (1994) 125.

[7] B. Sbarufatti, R. Falomo, A. Treves and J. Kotilainen, *Optical spectroscopy of BL Lacertae objects. Broad lines, companion galaxies, and redshift lower limits*, *Astron. Astrophys.* **457** (2006) 35.

[8] M. H. Ulrich, *Spectra of the stellar population in three objects related to BL Lacertae.*, *Astrophys. J. Lett.* **222** (1978) L3.

[9] S. L. Morris and M. J. Ward, *Spectrophotometry of active galaxies - I. The observations.*, *Mon. Not. R. astr. Soc.* **230** (1988) 639.

[10] E. Massaro, P. Giommi, C. Leto, P. Marchegiani, A. Maselli, M. Perri et al., *Roma-BZCAT: a multifrequency catalogue of blazars*, *Astron. Astrophys.* **495** (2009) 691.

[11] L. A. Crause, D. Gilbank, C. v. Gend, H. L. Worters, C. Sass, E. J. Kotze et al., *SpUpNIC (Spectrograph Upgrade: Newly Improved Cassegrain): a versatile and efficient low- to medium-resolution, long-slit spectrograph on the South African Astronomical Observatory's 1.9-m telescope*, *J. Astron. Telescopes, Instruments, and Systems* **5** (2019) 024007.

[12] H. Winkler, T. Kadiaka and F. van Wyk, *1E 0502-667: An AGN without narrow lines?*, in *High Energy Astrophysics in Southern Africa 2022*, p. 35, Dec., 2023.

[13] T. M. Brown, N. Baliber, F. B. Bianco, M. Bowman, B. Burleson, P. Conway et al., *Las Cumbres Observatory Global Telescope Network*, *Publ. astr. Soc. Pacific* **125** (2013) 1031.

[14] T. Jayasinghe, K. Z. Stanek, C. S. Kochanek, B. J. Shappee, T. W. S. Holoien, T. A. Thompson et al., *The ASAS-SN catalogue of variable stars III: variables in the southern TESS continuous viewing zone*, *Mon. Not. R. astr. Soc.* **485** (2019) 961.

[15] H. Winkler, *The extinction, flux distribution and luminosity of Seyfert 1 nuclei derived from UBV(RI)_C aperture photometry*, *Mon. Not. R. astr. Soc.* **292** (1997) 273.

[16] R. Bachev, T. Tripathi, A. C. Gupta, P. Kushwaha, A. Strigachev, A. Kurtenkov et al., *Intra-night optical flux and polarization variability of BL Lacertae during its 2020-2021 high state*, *Mon. Not. R. astr. Soc.* **522** (2023) 3018 [2304.03975].

PoS(HEASA2023)007